

# DeC and ADER: Similarities, Differences and a Unified Framework

Maria Han Veiga, and Philipp Öffner, and Davide Torlo  
 Institute of Mathematics, University of Zurich, Switzerland  
 Michigan Institute of Data Science, University of Michigan, USA

## Abstract

In this paper, we demonstrate that the ADER approach as it is used *inter alia* in [29] can be seen as a special interpretation of the deferred correction (DeC) method as introduced in [6]. By using this fact, we are able to embed ADER in a theoretical background of time integration schemes and prove the relation between the accuracy order and the number of iterations which are needed to reach the desired order. Finally, we can also investigate the stability regions for the ADER approach for different orders using several basis functions and compare them with the DeC ansatz.

## 1 Introduction

Very high-order methods have become rather ubiquitous in the field of numerical methods for hyperbolic partial differential equations. There are many methods which obtain an arbitrarily high-order in its spatial discretization, namely, discontinuous Galerkin [7, 18], spectral difference method [15, 8], etc. When considering time-dependent problems, the time integration must have the same order of convergence as of the spatial one, in order to formally guarantee the high order space-time convergence.

Explicit Runge–Kutta methods have long been used for its simplicity and ease of implementation. However, in the context of conservation laws, it is desirable for time integration to be Total Variation Diminishing (TVD), in order to avoid spurious oscillations. Runge-Kutta timestepping schemes that are TVD are the so called Strong Stability Preserving (TVD-SSP RK) schemes and they hit an accuracy barrier, as these methods cannot be higher than fourth order [22].

There are, however, timestepping methods which promise arbitrarily high accuracy, without the necessity to compute Butcher like coefficient tables, such as Deferred Correction [6], ADER [26], SBP [17] or (continuous or discontinuous) Galerkin approaches also in time.

The deferred correction method was first introduced in the context of ODEs, and later, formulated as a timestepping scheme for PDEs in conjunction with Finite Element ansatzes [1, 14]. The key idea of DeC is based on the Picard-Lindelf Theorem and especially on Picard iteration. In every iteration step, we decrease the error of the numerical solution until we reach a fixed bound / limit. Extension to implicit or semi-implicit variation exist [16] but we concentrate on the explicit version. From our point of view, some advantages of DeC compared with explicit RK are the possibility to use an FE ansatz in space and avoid the inversion of mass matrix to obtain a full discretization of a PDE as described in [1] or to obtain arbitrary high order time accuracy without computing the order conditions checks.

The ADER approach, introduced firstly in [26] and further developed in many other works, e.g. [5, 24, 29], remains quite elusive and misunderstood in the broad community of numerical analysis for hyperbolic problems, despite being able to achieve arbitrary high order in time without the well known barriers found in, for example, TVD-SSP RK.

The first ADER methods for linear hyperbolic equations were presented in [23, 26]. The (historical) ADER (Advection-Diffusion-Reaction) approach, described in the paper “ADER: Arbitrary High Order Godunov Approach” [24], extends what the method to nonlinear hyperbolic systems, achieving arbitrary high order accuracy both in time and space. The key ingredient of this approach is to consider a generalised Riemann Problem [25].

Later, in [5], a different formulation of ADER is presented, which can be interpreted as a space-time finite element method. This is the ADER approach that we consider in this paper, referring to it as the *modern ADER* (described in detail in section 2). Although used abundantly in many codes, the theoretical properties of ADER are not well studied. Some literature shows, for example, that for a linear homogeneous system, a finite number of iterations is sufficient to convergence [11]. However, questions on how to choose integration points, polynomial basis, are only addressed empirically up-to-our knowledge. Since DeC and the modern ADER are both iterative approaches, the questions that motivated this paper are the following:

1. Is there a connection between the ADER timestepping method and the DEC timestepping method? And if yes, what is this connection?
2. Does the connection between ADER and DEC help us study properties of the ADER scheme?

In order to address these questions, we first introduce the two methods considered. In section 2, we describe the ADER approach and, in section 3, the Deferred Correction method. Then, in section 4, we show that these two methods are very similar and that DEC can be written as an ADER scheme and vice versa. This connection is also verified through numerical experiments shown in section 5. Finally, we conclude the paper with a discussion in section 6.

## 2 The (Modern) ADER Approach

In the following section, we will give a short introduction about the ADER approach and how we understand it. Actually, it is an iterative process to obtain the numerical solution of a given space–time PDE. Therefore, we consider for simplicity the following scalar (non)linear hyperbolic problem

$$\partial_t u + \partial_x f(u) = 0. \quad (1)$$

Suppose that  $u(x, t)$  solves this equation under sufficient boundary and initial conditions. The main idea of the modern ADER is based on the variational formulation in the finite element context. We suppose to approximate the field  $u(x, t)$  in a set of space nodes  $\{x_i\}_{i=1}^I \subset \mathbb{R}$  and we denote with the vector  $\boldsymbol{\alpha}(t) = \{u(x_i, t)\}_{i=1}^I : \mathbb{R}^+ \rightarrow \mathbb{R}^I$  the semidiscretization in space of the function  $u$ <sup>1</sup>.

For the time discretization, we consider a time interval  $T^n := [t^n, t^n + \Delta t]$ , and we represent  $\boldsymbol{\alpha}(t)$  as a linear combination of basis functions in the time component  $t$ :

$$\boldsymbol{\alpha}(t) = \sum_{m=0}^M \phi_j(t) \boldsymbol{\alpha}^j = \underline{\phi}(t)^T \underline{\boldsymbol{\alpha}}, \quad (2)$$

where  $\underline{\phi} = [\phi_0, \dots, \phi_M]^T : T^n \rightarrow \mathbb{R}^{M+1}$  is the vector of time basis functions and  $\underline{\boldsymbol{\alpha}} = [\boldsymbol{\alpha}^0, \dots, \boldsymbol{\alpha}^M]^T \in \mathbb{R}^{(M+1) \times I}$  is the vector of coefficients related to the time basis functions for each degree of freedom in space. Typically,  $\underline{\phi}$  are Lagrange basis functions in some nodes

$$\{t_m\}_{m=0}^M \subset T^n, \quad (3)$$

e.g. equispaced, Gauss-Lobatto or Gauss-Legendre nodes.

Proceeding with the weak formulation in time, we consider a smooth test function  $\psi(t) : \mathbb{R} \rightarrow \mathbb{R}$  and we integrate over some interval  $T^n$ .

We consider, from now on, only the time derivatives of the hyperbolic equation (1). In other words, we can say that, through the method of lines, we make a splitting in space and time because the ADER approach will be used as the time integration method and it will be fully explicit. For the space discretisation, one can

---

<sup>1</sup>By switching from the PDE formulation to the ODE setting, we change also the used notation. Here,  $u$  is used in the PDE case and  $\alpha$  when speaking about an ODE.

use their favorite numerical scheme, *inter alia* discontinuous Galerkin (DG), flux reconstruction (FR), finite volume (FV) or ENO/WENO space which finally yield to the different ADER representation like ADER–WENO or ADER–DG that can be found in literature. Additionally, we will not suffer from any other issues like accuracy reduction or similar if using one the above described space methods.

We consider, thus, the function  $F : \mathbb{R}^I \rightarrow \mathbb{R}^I$  to be the semi-discrete operator in space for all the degrees of freedom, which is given by the chosen spatial scheme. We can just focus then on the resulting system of ODEs for  $\boldsymbol{\alpha} : [0, T] \rightarrow \mathbb{R}^I$

$$\partial_t \boldsymbol{\alpha} + F(\boldsymbol{\alpha}) = 0. \quad (4)$$

Its variational form in time is given by

$$\int_{T^n} \psi(t) \partial_t \boldsymbol{\alpha}(t) dt + \int_{T^n} \psi(t) F(\boldsymbol{\alpha}(t)) dt = 0, \quad \forall \psi : T^n \rightarrow \mathbb{R}. \quad (5)$$

Now, we replace the unknown with its reconstruction and we choose the test functions to be the same as the basis functions. This results in the following definition of the operator  $\mathcal{L}^2 : \mathbb{R}^{(M+1) \times I} \rightarrow \mathbb{R}^{(M+1) \times I}$

$$\mathcal{L}^2(\boldsymbol{\alpha}) := \int_{T^n} \underline{\phi}(t) \partial_t \underline{\phi}(t)^T \boldsymbol{\alpha} dt + \int_{T^n} \underline{\phi}(t) F(\underline{\phi}(t)^T \boldsymbol{\alpha}) dt = 0. \quad (6)$$

Integrating by parts yields

$$\mathcal{L}^2(\boldsymbol{\alpha}) = \underline{\phi}(t^{n+1}) \underline{\phi}(t^{n+1})^T \boldsymbol{\alpha} - \underline{\phi}(t^n) \boldsymbol{\alpha}(t^n) - \int_{T^n} \partial_t \underline{\phi}(t) \underline{\phi}(t)^T dt \boldsymbol{\alpha} + \int_{T^n} \underline{\phi}(t) F(\underline{\phi}(t)^T \boldsymbol{\alpha}) dt = 0. \quad (7)$$

Now, we replace the integrals by quadratures. The quadrature nodes can coincide (or not) with the ones defining the Lagrange polynomials<sup>2</sup>. We denote them as  $\{t_z^q\}_{z=0}^Z \subset T^n$  and with respective weights  $\{w_z\}_{z=0}^Z$ . We choose the weights, the nodes and the basis functions to be scaled for the interval  $[0, 1]$ , so that we explicitly highlight the presence of  $\Delta t = t^{n+1} - t^n$ . The integration terms reduce to

$$\begin{aligned} \int_{T^n} \partial_t \underline{\phi}(t) \underline{\phi}(t)^T dt \boldsymbol{\alpha} &\approx \sum_{z=0}^Z w_z \partial_t \underline{\phi}(t_z^q) \underline{\phi}(t_z^q)^T \boldsymbol{\alpha} \\ \int_{T^n} \underline{\phi}(t) F(\underline{\phi}(t)^T \boldsymbol{\alpha}) dt &\approx \Delta t \sum_{z=0}^Z w_z \underline{\phi}(t_z^q) F(\underline{\phi}(t_z^q)^T \boldsymbol{\alpha}). \end{aligned} \quad (8)$$

Then, the approximation of (7) yields, for every test function indexed by  $m = 0, \dots, M$

$$\phi_m(t^{n+1}) \underline{\phi}(t^{n+1})^T \boldsymbol{\alpha} - \sum_{z=0}^Z w_z \partial_t \underline{\phi}(t_z^q) \underline{\phi}(t_z^q)^T \boldsymbol{\alpha} = \phi_m(t^n) \boldsymbol{\alpha}(t^n) - \Delta t \sum_{z=0}^Z w_z \underline{\phi}(t_z^q) F(\underline{\phi}(t_z^q)^T \boldsymbol{\alpha}). \quad (9)$$

This is a system of  $M + 1$  equations with  $M + 1$  unknowns for every ODE of the system (4). Actually, what is expressed here is nothing more than a classical collocation method, c.f. [28], or a high order implicit RK method. The order depends on the used quadrature rule. Using, as an example, Gauss–Legendre or Gauss–Lobatto nodes both for the definition of the basis functions and the quadrature nodes results in a high order quadrature formula. One can also use different points for the quadrature and the basis functions, resulting in more varieties of this scheme.

We can rewrite the system (9) in a matrix–fashioned way, using the mass matrix  $\underline{\underline{M}} \in \mathbb{R}^{(M+1) \times (M+1)}$ , given by

$$\underline{\underline{M}}_{m,l} := \phi_m(t^{n+1}) \phi_l(t^{n+1}) - \sum_{z=0}^Z \partial_t \phi_m(t_z^q) \phi_l(t_z^q) w_z \quad (10)$$

<sup>2</sup>In this work we choose the quadrature nodes as equidistant, Gauss–Lobatto or Gauss–Legendre nodes. However, in many application of ADER, Gauss–Legendre nodes are the typical choice to guarantee the exactness of the integration.

and the right-hand side functional  $\underline{r}(\underline{\alpha}) : \mathbb{R}^{(M+1) \times I} \rightarrow \mathbb{R}^{(M+1) \times I}$ , given by

$$\underline{r}(\underline{\alpha})_m := \phi_m(t^n) \alpha(t^n) - \Delta t \sum_{z=0}^Z w_z \phi_m(t_z^q) F(\phi(t_z^q)^T \underline{\alpha}), \quad m = 0, \dots, M+1. \quad (11)$$

We have brought on the right-hand side of (9) the nonlinear terms and the explicit ones, while keeping the linear terms on the left-hand side. Finally, our system to be solved is given by

$$\underline{\underline{M}} \underline{\alpha} = \underline{r}(\underline{\alpha}) \iff \mathcal{L}^2(\underline{\alpha}) := \underline{\underline{M}} \underline{\alpha} - \underline{r}(\underline{\alpha}) \stackrel{!}{=} 0. \quad (12)$$

This equation is nothing else than a fixed-point problem. Its solution will give us an  $(M+1)$ th order accurate solution in time. It cannot be directly solved when nonlinear fluxes are present, but it can be solved under certain assumptions with an iterative process in  $\underline{\alpha}$ . Defining the starting guess as  $\underline{\alpha}^{(0)} := [\alpha(t^n), \dots, \alpha(t^n)]^T$ , the algorithm proceeds iteratively as follows

$$\underline{\alpha}^{(k)} = \underline{\underline{M}}^{-1} \underline{r}(\underline{\alpha}^{(k-1)}), \quad k = 1, \dots, K. \quad (13)$$

Several questions arise automatically for (13), such as, how is the convergence of the method influenced by the mass matrix  $\underline{\underline{M}}$  and, hence, by the node placement? By re-interpreting the new ADER approach into the DeC framework in section 4, we can answer these and more questions, thanks to the definition of the  $\mathcal{L}^2$  operator in (12). This serves as a connection to the DeC procedure. Before introducing the DeC method, we give the following simple example to get more familiar with the ADER method.

**Example 2.1.** *2<sup>nd</sup> order ADER method for ODEs* Let us demonstrate a concrete example of the methodology described above, considering a simple scalar ODE:

$$\alpha'(t) + F(\alpha) = 0, \quad (14)$$

with  $\alpha : [0, T] \rightarrow \mathbb{R}$ .

Let us consider the timestep interval  $[t^n, t^{n+1}]$ , rescaled to  $[0, 1]$ . The time interpolation nodes and the quadrature nodes are given by Gauss-Legendre points (in the interval  $[0, 1]$ ) and respective quadrature weights.

$$t_q = (t_q^0, t_q^1) = (t^0, t^1) = \left( \frac{\sqrt{3}-1}{2\sqrt{3}}, \frac{\sqrt{3}+1}{2\sqrt{3}} \right), \quad \underline{w} = (1/2, 1/2).$$

The time basis is given by Lagrange interpolation polynomials built on the nodes  $t^q$ .

$$\underline{\phi}(t) = (\phi_0(t), \phi_1(t)) = \left( \frac{t-t^1}{t^0-t^1}, \frac{t-t^0}{t^1-t^0} \right).$$

Then, the mass matrix is given by

$$\underline{\underline{M}}_{m,l} = \phi_m(1) \phi_l(1) - \phi'_m(t^l) w_l, \quad m, l = 0, 1,$$

thanks to the definition of the Lagrange polynomials.

$$\underline{\underline{M}} = \begin{pmatrix} 1 & \frac{\sqrt{3}-1}{2} \\ -\frac{\sqrt{3}+1}{2} & 1 \end{pmatrix}.$$

The right hand side is given by<sup>3</sup>

---

<sup>3</sup>Note that the quadrature process is greatly simplified because of the choice of Gauss-Legendre nodes both for the quadrature and the Lagrangian basis functions in (10) and (11).

$$r(\underline{\alpha})_m = \alpha(0)\phi_m(0) - \Delta t F(\alpha(t^m))w_m, \quad m = 0, 1.$$

$$\underline{r}(\underline{\alpha}) = \alpha(0)\underline{\phi}(0) - \Delta t \begin{pmatrix} F(\alpha(t^1))w_1 \\ F(\alpha(t^2))w_2 \end{pmatrix}.$$

Then, the coefficients  $\underline{\alpha}$  are given by

$$\underline{\alpha}^{(k+1)} = \underline{\underline{M}}^{-1} \underline{r}(\underline{\alpha}^{(k)}).$$

Finally, use  $\underline{\alpha}^{(k+1)}$  to reconstruct the solution at the time step  $t^{n+1}$ :

$$\alpha^{n+1} = \underline{\phi}(1)^T \underline{\alpha}^{(k+1)}.$$

## 2.1 Historical ADER

In the community, the term ADER is often associated with the historical approach. In order to establish the difference between the modern version of ADER and the historical one, we explain the procedure, as introduced in [24], highlighting the key differences between the two methods.

Solving the same problem as in (1), let us consider  $t^n$  as starting time and suppose that we have at our disposal the cell averages:  $u_i(t^n)$ , for  $i$  indexing control volumes  $V$ .

The method consists of three steps:

1. reconstruction of pointwise values from cell averages (using some reconstruction function  $\mathcal{R}$ )

$$\mathcal{R}(u_{i-k}, \dots, u_{i+l}, t^n) = u(x, t^n), \quad x \in V_i,$$

2. solution of the generalized Riemann problem at the cell interfaces,
3. evaluation of the intercell flux to be used in the conservative scheme.

The main difference is in step two. In order to solve the generalised Riemann problem at the cell interfaces (for all local times  $\tau := t - t^n$ ), one writes the Taylor expansion of the interface state in time

$$u(x_{i+1/2}, \tau) = u(x_{i+1/2}, 0^+) + \sum_{k=1}^m \left[ \partial_t^{(k)} u(x_{i+1/2}, 0^+) \right] \frac{\tau^k}{k!} \quad (15)$$

Note that the leading term,  $u(x_{i+1/2}, 0^+)$ , accounts for interactions with the boundary extrapolated values  $u_L(x_{i+1/2})$  and  $u_R(x_{i+1/2})$ , and it is the Godunov state of the conventional (piece-wise constant data) Riemann Problem. Typically, an exact or approximate Riemann solver is used to provide the first term of the approximation.

The next terms are higher order corrections to the 0th Godunov state. The high order derivatives in time are replaced by derivatives in space by means of the Lax–Wendroff procedure [13].

As in [27], the space derivatives  $\partial_x^{(k)} u(x, t)$  of the solution at  $(x - x_{i+1/2}, \tau) = 0$  can be evaluated as the Godunov states of the following linearized generalized Riemann Problem:

$$\begin{aligned} \partial_t u^{(k)} + A(u(x_{i+1/2}, 0^+)) \partial_x u^{(k)} &= 0, \\ u^{(k)}(x, 0) &= \begin{cases} \partial_x^{(k)} u_L(x_{i+1/2}), & x < x_{i+1/2}, \\ \partial_x^{(k)} u_R(x_{i+1/2}), & x > x_{i+1/2}. \end{cases} \end{aligned} \quad (16)$$

The initial condition for the Riemann Problem (16) above is given by differentiating the high-order reconstruction polynomial with respect to  $x$ . Having all derivatives in terms of their spatial component, the Taylor expansion (15) can be evaluated as

$$u(x_{i+1/2}, \tau) = a_0 + a_1\tau + a_2\tau^2 + \dots + a_m\tau^m \quad (17)$$

for  $a_j$  containing all the constants not depending on  $\tau$ . This expression approximates the interface state for  $0 \leq \tau \leq \Delta t$  to  $(m+1)$ -th order of accuracy.

Finally, to evaluate the numerical flux (now in time as well), an appropriate Gaussian rule is used:

$$\hat{F}_{i+1/2} = \sum_{q=0}^M F(u(x_{i+1/2}, t^q \Delta t)) \omega_q,$$

where  $t^q, \omega_q$  are nodes and weights of the quadrature rule, and  $M+1$  the number of nodes.

## 2.2 ADER space-time DG

Up to now, we have presented the modern and historical ADER approach from our point of view. However, to clarify again that our description of the modern ADER used in 2 is indeed equivalent with the one used *inter alia* in [29], we focus again on it. We hope that the understanding for ADER will be much simpler with this different perspective.

We follow now [29] where ADER is presented as a space-time DG approach. They use time and space test functions, which are the tensor products of basis functions in time and basis functions in space. We can write their formulation in our setting. Hence, we define the new basis functions

$$\theta_{pq}(x, t) := \Phi_p(x) \phi_q(t), \quad (18)$$

where  $\Phi$  are the basis functions in space and  $\phi$  are the basis functions in time. With the Einstein summation notation, the reconstruction variable is

$$u(x, t) = u^{pq} \theta_{pq}(x, t) = \sum_p \sum_q u^{pq} \Phi_p(x) \phi_q(t). \quad (19)$$

Let us consider a hyperbolic problem given as

$$\partial_t u(x, t) + \nabla \cdot F(u(x, t)) = 0, \quad x \in \Omega \subset \mathbb{R}^d, t > 0 \quad (20)$$

with appropriate initial and boundary conditions. We consider the weak solution of (20) in space-time. Let us define a space-time cell,  $T^n \times V_i$ , given by the tensor product of a timestep  $T^n$  and a volume cell  $V_i \subset \mathbb{R}^d$ . We multiply (20) by test function  $\theta_{rs}(x, t)$  and integrate over the defined control volume:

$$\int_{T^n \times V_i} \theta_{rs}(x, t) \partial_t \theta_{pq}(x, t) u^{pq} dx dt + \int_{T^n \times V_i} \theta_{rs}(x, t) \nabla \cdot F(\theta_{pq}(x, t) u^{pq}) dx dt = 0. \quad (21)$$

We also introduce the following definitions

$$u^q(x) = \Phi_p(x) u^{pq}, \quad u^p(t) := \phi_q(t) u^{pq}. \quad (22)$$

Now, we apply Gauss theorem (e.g. integration by parts) in time and space and obtain

$$0 = \int_{V_i} \Phi_r(x) \Phi_p(x) dx \left( \phi_s(t^{n+1}) \phi_q(t^{n+1}) u^{pq} - \phi_s(t^n) u^p(t^n) - \int_{T^n} \partial_t \phi_s(t) \phi_q(t) dt u^{pq} \right) + \int_{T^n} \phi_s(t) \phi_q(t) dt \left( \int_{\partial V_i} \Phi_r(x) \mathcal{G}(u^{q,+}(x), u^{q,-}(x)) \cdot \mathbf{n} dx - \int_{V_i} \nabla \cdot \Phi_r(x) F(u^q(x)) dx \right), \quad (23)$$

where  $\mathcal{G}$  is a classical numerical two-point flux,  $u^+$  is the value of  $u$  inside  $V_i$  and  $u^-$  is the value of  $u$  in the neighboring cell and the normal vector  $\mathbf{n}$  is pointing outwards. We define the spatial mass matrix and the time mass matrix as

$$\underline{\underline{\mathbf{M}}}_{rp}^x := \int_{V_i} \Phi_r(x) \Phi_p(x) dx, \quad \underline{\underline{\mathbf{M}}}_{sq}^t := \int_{T^n} \phi_s(t) \phi_q(t) dt. \quad (24)$$

Splitting as done in (9) into a linear left-hand side and a non-linear right-hand side, we obtain

$$\begin{aligned} \underline{\underline{\mathbf{M}}}_{rp}^x \left( \phi_s(t^{n+1}) \phi_q(t^{n+1}) - \int_{T^n} \partial_t \phi_s(t) \phi_q(t) dt \right) u^{pq} = \\ \underline{\underline{\mathbf{M}}}_{rp}^x \phi_s(t^n) u^p(t^n) - \underline{\underline{\mathbf{M}}}_{sq}^t \left( \int_{\partial V_i} \Phi_r(x) \mathcal{G}(u^{q,+}(x), u^{q,-}(x)) \cdot \mathbf{n} dx - \int_{V_i} \nabla \cdot \Phi_r(x) F(u^q(x)) dx \right). \end{aligned} \quad (25)$$

Using the Picard iteration process we obtain, again

$$\underline{\underline{\mathbf{M}}}_{rspq} u^{pq,(k+1)} = \underline{\underline{\mathbf{r}}}(\underline{\underline{\mathbf{u}}})_{rs}, \quad (26)$$

where

$$\underline{\underline{\mathbf{M}}}_{rspq} := \underline{\underline{\mathbf{M}}}_{rp}^x \left( \phi_s(t^{n+1}) \phi_q(t^{n+1}) - \int_{T^n} \partial_t \phi_s(t) \phi_q(t) dt \right), \quad (27)$$

$$\underline{\underline{\mathbf{r}}}(\underline{\underline{\mathbf{u}}})_{rs} := \underline{\underline{\mathbf{M}}}_{rp}^x \phi_s(t^n) u^p(t^n) - \underline{\underline{\mathbf{M}}}_{sq}^t \left( \int_{\partial V_i} \Phi_r(x) \mathcal{G}(u^{q,+}(x), u^{q,-}(x)) \cdot \mathbf{n} dx - \int_{V_i} \nabla \cdot \Phi_r(x) F(u^q(x)) dx \right). \quad (28)$$

**Remark 2.2.** We presented here in detail the ADER–DG method. Considering the (27), one notice that the full space–time matrix, actually depends on several different mass matrices, i.e., on  $\underline{\underline{\mathbf{M}}}_{rp}^x$  and on  $\underline{\underline{\mathbf{M}}}_{sq}^t$ . Changes in the space discretization affect only the space discretisation matrix  $\underline{\underline{\mathbf{M}}}_{rp}^x$ , one can, for example, consider different schemes like Flux Reconstruction which are working with the differential formulation of the PDE. Nevertheless, the time–integration structure of the matrix (27) given by the ADER approach will stay the same. That is why we can consider the ADER to be a time integration method.

### 3 Deferred Correction Methods

In this section, we focus on the **Deferred Correction (DeC)** method which was introduced by Dutt et al. [6] and then reinterpreted by Abgrall [1]. It is an explicit, arbitrary high order method for ODEs but further extensions of DeC, including implicit, semi-implicit or modified Patankar versions, can be found nowadays in the literature [4, 16, 19].

Since we want to embed the modern ADER approach into this framework, we focus only on the explicit version. Therefore, we use the notation of DeC introduced by Abgrall in [1] because, in our opinion, it is more convenient to prove accuracy than in previous works [6, 4, 14]. Actually, Abgrall focuses on DeC as a time integration scheme in the context of finite element methods. In particular, when using continuous Galerkin schemes for the space discretization and applying RK methods, a sparse mass matrix has to be inverted. Through the DeC approach, one can avoid the mass matrix inversion.

The main core of all the DeC algorithms is the same and it is based on the Picard-Lindelöf theorem in the continuous setting. The theorem states the existence and uniqueness of solutions for ODEs. The classical proof makes use of the so-called Picard iterations to minimize the error and to prove the convergence of the method, which is nothing else than a fixed-point problem. The foundation of DeC relies on mimicking the Picard iterations and the fixed-point iteration process at the discrete level.

Here, we see already some connection between the two approaches. Indeed, the approximation error decreases with several iteration steps. For the description of DeC, let us consider the system of ODEs as in (4)

$$\alpha'(t) + F(\alpha) = 0,$$

with  $\alpha : [0, T] \rightarrow \mathbb{R}^I$ . Abgrall introduces two operators:  $\mathcal{L}^1$  and  $\mathcal{L}^2$ . The  $\mathcal{L}^1$  operator represents a low-order easy-to-solve numerical scheme, e.g. the explicit Euler method, and  $\mathcal{L}^2$  is a high-order operator that can present difficulties in its practical solution, e.g. an implicit RK scheme or a collocation method. We use here on purpose the  $\mathcal{L}^1, \mathcal{L}^2$  nomenclature since we will see that actually this is the key point in the connection.

The DeC method can be written as a combination of these two operators.

Given a timeinterval  $[t^n, t^{n+1}]$  we subdivide it into  $M$  subintervals  $\{[t^{n,m-1}, t^{n,m}]\}_{m=1}^M$ , where  $t^{n,0} = t^n$  and  $t^{n,M} = t^{n+1}$  and we mimic for every subinterval  $[t^0, t^m]$  the Picard–Lindelöf theorem for both operators  $\mathcal{L}^1$  and  $\mathcal{L}^2$ . We drop the dependency on the timestep  $n$  for subimesteps  $t^{n,m}$  and substates  $\alpha^{m,n}$  as denoted in Figure 1.

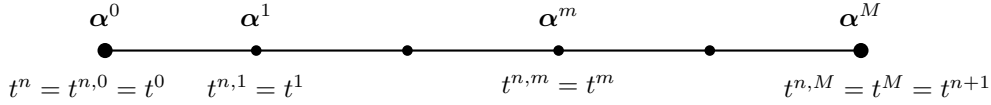


Figure 1: Figure: divided time interval

Then, the  $\mathcal{L}^2$  operator is given by

$$\mathcal{L}^2(\alpha^0, \dots, \alpha^M) := \begin{cases} \alpha^M - \alpha^0 - \int_{t^0}^{t^M} \mathcal{I}_M(F(\alpha^0), \dots, F(\alpha^M)) = \alpha^M - \alpha^0 - \sum_{r=0}^M \int_{t^0}^{t^M} F(\alpha^r) \varphi_r(s) ds \\ \vdots \\ \alpha^1 - \alpha^0 - \int_{t^0}^{t^1} \mathcal{I}_M(F(\alpha^0), \dots, F(\alpha^M)) = \alpha^1 - \alpha^0 - \sum_{r=0}^M \int_{t^0}^{t^1} F(\alpha^r) \varphi_r(s) ds \end{cases} . \quad (29)$$

Here, the term  $\mathcal{I}_M$  denotes an interpolation polynomial of order  $M$  evaluated at the points  $\{t^{n,r}\}_{r=0}^M$ . In particular, we use Lagrange polynomials  $\{\varphi_r\}_{r=0}^M$ , where  $\varphi_r(t^{n,m}) = \delta_{r,m}$  and  $\sum_{r=0}^M \varphi_r(s) \equiv 1$  for any  $s \in [0, 1]$ . Using these properties, we can actually compute the integral of the interpolants, thanks to a quadrature rule in the same points  $\{t^m\}_{m=0}^M$  with weights  $\theta_r^m := \int_{t^n}^{t^{n,m}} \varphi_r(s) ds$ . We can rewrite

$$\mathcal{L}^2(\alpha^0, \dots, \alpha^M) = \begin{cases} \alpha^M - \alpha^0 - \Delta t \sum_{r=0}^M \theta_r^M F(\alpha^r) \\ \vdots \\ \alpha^1 - \alpha^0 - \Delta t \sum_{r=0}^M \theta_r^1 F(\alpha^r) \end{cases} . \quad (30)$$

The  $\mathcal{L}^2$  operator represents an  $(M+1)$ th order numerical scheme (collocation method) if set equal to zero, i.e.,  $\mathcal{L}^2(\alpha^0, \dots, \alpha^M) = 0$ . Unfortunately, the resulting scheme is implicit and, further, the terms  $F$  may be nonlinear. Because of this, the only  $\mathcal{L}^2 = 0$  formulation is not explicit and more efforts have to be made to solve it.

For this purpose, we introduce a simplification of the  $\mathcal{L}^2$  operator. Instead of using a quadrature formula at the points  $\{t^m\}_{m=0}^M$  we evaluate the integral in equation (29) applying the left Riemann sum. The resulting operator  $\mathcal{L}^1$  is given by the forward Euler discretization for each state  $\alpha^m$  in the timeinterval, i.e.,

$$\mathcal{L}^1(\alpha^0, \dots, \alpha^M) := \begin{cases} \alpha^M - \alpha^0 - \beta^M \Delta t F(\alpha^0) \\ \vdots \\ \alpha^1 - \alpha^0 - \beta^1 \Delta t F(\alpha^0) \end{cases} . \quad (31)$$

with coefficients  $\beta^m := \frac{t^m - t^0}{t^M - t^0}$ .

To simplify the notation and to describe DeC, as before, we introduce the vector of states for the variable  $\alpha$  at all subimesteps

$$\underline{\alpha} := (\alpha^0, \dots, \alpha^M) \in \mathbb{R}^{M \times I}, \text{ such that} \quad (32)$$

$$\mathcal{L}^1(\underline{\alpha}) := \mathcal{L}^1(\alpha^0, \dots, \alpha^M) \text{ and } \mathcal{L}^2(\underline{\alpha}) := \mathcal{L}^2(\alpha^0, \dots, \alpha^M). \quad (33)$$



Now, the DeC algorithm uses a combination of the  $\mathcal{L}^1$  and  $\mathcal{L}^2$  operators to provide an iterative procedure. The aim is to recursively approximate  $\underline{\alpha}^*$ , the numerical solution of the  $\mathcal{L}^2(\underline{\alpha}^*) = 0$  scheme, similarly to the Picard iterations in the continuous setting. The successive states of the iteration process will be denoted by the superscript  $(k)$ , where  $k$  is the iteration index, e.g.  $\underline{\alpha}^{(k)} \in \mathbb{R}^{M \times I}$ . The total number of iterations (also called correction steps) is denoted by  $K$ . To describe the procedure, we have to refer to both the  $m$ -th subimestep and the  $k$ -th iteration of the DeC algorithm. We will indicate the variable by  $\alpha^{m,(k)} \in \mathbb{R}^I$ . Finally, the DeC method can be written as

### DeC Algorithm

$$\begin{aligned}\alpha^{0,(k)} &:= \alpha(t^n), \quad k = 0, \dots, K, \\ \alpha^{m,(0)} &:= \alpha(t^n), \quad m = 1, \dots, M \\ \mathcal{L}^1(\underline{\alpha}^{(k)}) &= \mathcal{L}^1(\underline{\alpha}^{(k-1)}) - \mathcal{L}^2(\underline{\alpha}^{(k-1)}) \text{ with } k = 1, \dots, K,\end{aligned}\tag{34}$$

where  $K$  is the number of iterations that we want to compute. Using the procedure (34), we need, in particular, as many iterations as the desired order of accuracy, i.e.,  $K = M + 1$ . Notice that, in every step, we solve the equations for the unknown variables  $\underline{\alpha}^{(k)}$  which appears only in the  $\mathcal{L}^1$  formulation, the operator that can be easily inverted. Conversely,  $\mathcal{L}^2$  is only applied to already computed predictions of the solution  $\underline{\alpha}^{(k-1)}$ . Therefore, the scheme 34 is completely explicit and arbitrary high order as stated in [1] with the following proposition.

**Proposition 3.1.** *Let  $\mathcal{L}^1$  and  $\mathcal{L}^2$  be two operators defined on  $\mathbb{R}^{M \times I}$ , which depend on the discretization scale  $\Delta = \Delta t$ , such that*

- $\mathcal{L}^1$  is coercive with respect to a norm, i.e.,  $\exists \gamma_1 > 0$  independent of  $\Delta$ , such that for any  $\underline{\alpha}, \underline{\mathbf{d}}$  we have that

$$\gamma_1 \|\underline{\alpha} - \underline{\mathbf{d}}\| \leq \|\mathcal{L}^1(\underline{\alpha}) - \mathcal{L}^1(\underline{\mathbf{d}})\|,$$

- $\mathcal{L}^1 - \mathcal{L}^2$  is Lipschitz with constant  $\gamma_2 > 0$  uniformly with respect to  $\Delta$ , i.e., for any  $\underline{\alpha}, \underline{\mathbf{d}}$

$$\|(\mathcal{L}^1(\underline{\alpha}) - \mathcal{L}^2(\underline{\alpha})) - (\mathcal{L}^1(\underline{\mathbf{d}}) - \mathcal{L}^2(\underline{\mathbf{d}}))\| \leq \gamma_2 \Delta \|\underline{\alpha} - \underline{\mathbf{d}}\|.$$

We also assume that there exists a unique  $\underline{\alpha}_\Delta^*$  such that  $\mathcal{L}^2(\underline{\alpha}_\Delta^*) = 0$ . Then, if  $\eta := \frac{\gamma_2}{\gamma_1} \Delta < 1$ , the DeC is converging to  $\underline{\alpha}^*$  and after  $k$  iterations the error  $\|\underline{\alpha}^{(k)} - \underline{\alpha}^*\|$  is smaller than  $\eta^k \|\underline{\alpha}^{(0)} - \underline{\alpha}^*\|$ .

Proofs of this proposition and of the hypotheses of the proposition for operators  $\mathcal{L}^1$  and  $\mathcal{L}^2$  such as (31) and (30) can be found in [1, 2, 19].

The condition for  $\eta$  comes actually from the fixed-point theorem and has to be guaranteed that the iterative process converges. Before, we focus on the relation between DeC and ADER we give the following remark.

**Remark 3.2.** • *In the  $\mathcal{L}^1$  operator, one can use higher order time integration methods than the explicit Euler method. In principle, this increases the convergence rate in the iteration process. However, an accuracy drop down can be observed in some cases. This is due to the fact that the smoothness of the error is not given anymore, c.f. [4].*

- *In our description of DeC both endpoints are included. However, also Gauss-Legendre nodes like in example 2.1 can be used. Then, the approximation at the endpoint is done via extrapolation, see [6].*
- *Finally, any DeC method can be interpreted as a RK scheme [4]. The main difference between RK and DeC is that the latter gives a general approach to the time discretization and does not require a specification of the coefficients for every order of accuracy.*

## 4 Relation between DeC and ADER

What we see up to now was a repetition of the DeC and ADER approaches. Both are based on an iterative procedure and mainly the foundation is given by the same fixed–point iteration method. In the following, we point out the relation between these two methods, namely, we show how ADER can be expressed as DeC and vice versa. This relation can be used to prove a new theoretical result for the ADER algorithm. The number of iterations needed to the Picard process can be chosen equal to the accuracy order we aim to reach. This result can be used in a general setting, providing few hypotheses on the operators, extending the result of [11].

### 4.1 ADER as DeC

First, we start to show how the modern ADER can be put into the DeC framework which we have described in section 3. Therefore, let us rewrite the  $\mathcal{L}^2$  operator from section 2. It is given in equation (7) and (12). It is

$$\mathcal{L}^2(\underline{\alpha}) := \underline{\underline{M}}\underline{\alpha} - r(\underline{\alpha}),$$

where  $\underline{\underline{M}}$  is the previously defined invertible mass matrix. For the DeC algorithm 34, we need further an low–order explicit operator. For the ADER, we choose the same low order operator of the DeC, namely,

$$\mathcal{L}^1(\underline{\alpha}) := \underline{\underline{M}}\underline{\alpha} - r(\underline{\alpha}(t^n)). \quad (35)$$

Actually, we have to mention that this operator is not really unique and can be defined in different ways, since all the information is already included in the  $\mathcal{L}^2$  operator for the ADER–DeC approach (see remark 4.1). Nevertheless, the choice of (35) is useful for the hypotheses of the proposition 3.1, because, in this way, the difference of the two operators will be Lipschitz continuous.

Then, we obtain the ADER-DeC algorithm:

$$\mathcal{L}^1(\underline{\alpha}^{(k)}) = \mathcal{L}^1(\underline{\alpha}^{(k-1)}) - \mathcal{L}^2(\underline{\alpha}^{(k-1)}), \quad k = 1, \dots, K,$$

defining  $\underline{\alpha}^{(k),0} = \underline{\alpha}(t^n)$ ,  $\forall k$ . Hence, we can explicitly write it as

$$\begin{aligned} \underline{\underline{M}}\underline{\alpha}^{(k+1)} - r(\underline{\alpha}^{(k+1)}(t^n)) - \underline{\underline{M}}\underline{\alpha}^{(k)} + r(\underline{\alpha}^{(k)}(t^n)) + \underline{\underline{M}}\underline{\alpha}^{(k)} - r(\underline{\alpha}^{(k)}) &= 0 \\ \underline{\underline{M}}\underline{\alpha}^{(k+1)} - r(\underline{\alpha}^{(k)}) &= 0. \end{aligned}$$

which is nothing more than the discrete fixed–point problem in equation (12).

**Remark 4.1.** *The operator  $\mathcal{L}^2$  already comprises the information needed in the fixed–point iteration. Nevertheless, the  $\mathcal{L}^1$  operator serves us to easily prove the convergence up to the required order of accuracy of the process. Finally, we like to mention that one can also define the operators as*

$$\begin{cases} \mathcal{L}^1(\underline{\alpha}) := \underline{\alpha} - \underline{\underline{M}}^{-1}r(\underline{\alpha}(t^n)), \\ \mathcal{L}^2(\underline{\alpha}) := \underline{\alpha} - \underline{\underline{M}}^{-1}r(\underline{\alpha}). \end{cases} \quad (36)$$

*and obtain an analog result. We use this expression when demonstrating the accuracy property in subsection 4.3.*

### 4.2 DeC as ADER

Here, we will show that the DeC scheme can be derived from the ADER method. The essential difference is the choice of appropriate basis functions. This is mainly related to the definition of the  $\mathcal{L}^2$  operator in the DeC framework. If we rewrite (29)

$$\mathcal{L}^2(\underline{\alpha}) := \begin{cases} \underline{\alpha}^M - \underline{\alpha}^0 - \int_{t^0}^{t^M} \mathcal{I}_M(F(\underline{\alpha}^0), \dots, F(\underline{\alpha}^M)) = \underline{\alpha}^M - \underline{\alpha}^0 - \sum_{r=0}^M \int_{t^0}^{t^M} F(\underline{\alpha}^r) \varphi_r(t) dt \\ \vdots \\ \underline{\alpha}^1 - \underline{\alpha}^0 - \int_{t^0}^{t^1} \mathcal{I}_M(F(\underline{\alpha}^0), \dots, F(\underline{\alpha}^M)) = \underline{\alpha}^1 - \underline{\alpha}^0 - \sum_{r=0}^M \int_{t^0}^{t^1} F(\underline{\alpha}^r) \varphi_r(t) dt \end{cases} .$$

and focus on the  $m$ -th line, which reads

$$\boldsymbol{\alpha}^m - \boldsymbol{\alpha}^0 - \sum_{r=0}^M F(\boldsymbol{\alpha}^r) \int_{t^0}^{t^m} \varphi_r(t) dt = 0,$$

we can rewrite the  $\mathcal{L}^2$  operator in the following form

$$\chi_{[t^0, t^m]}(t^m) \boldsymbol{\alpha}^m - \chi_{[t^0, t^m]}(t_0) \boldsymbol{\alpha}^0 - \sum_{r=0}^M F(\boldsymbol{\alpha}^r) \int_{t^0}^{t^m} \chi_{[t^0, t^m]}(t) \varphi_r(t) dt = 0, \quad (37)$$

where  $\chi_{[t^0, t^m]}$  is the characteristic function in the interval  $[t^0, t^m]$ , i. e.,

$$\chi_{[t^0, t^m]}(t) = \begin{cases} 1, & \text{if } t \in [t^0, t^m], \\ 0, & \text{else.} \end{cases} \quad (38)$$

Therefore, we can actually include the integration also for the first two terms of equation (37), resulting in

$$\int_{t^0}^{t^M} \chi_{[t^0, t^m]}(t) \partial_t (\boldsymbol{\alpha}(t)) dt - \sum_{r=0}^M F(\boldsymbol{\alpha}^r) \int_{t^0}^{t^M} \chi_{[t^0, t^m]}(t) \varphi_m(t) dt = 0, \quad (39)$$

$$\int_{T^n} \psi_m(t) \partial_t \boldsymbol{\alpha}(t) dt - \int_{T^n} \psi_m(t) F(\boldsymbol{\alpha}(t)) dt = 0, \quad (40)$$

where  $\psi_m(t) = \chi_{[t^0, t^m]}(t)$  are the chosen test functions.

If we compare (40) with the beginning ADER formulation (5) and (6), we notice that they differ just in the choice of the test functions. If for the ADER approach we chose test functions to be the basis functions, in the DeC method we considered different test functions.

Inserting this in the DeC algorithm, we obtain

$$\chi_{[t^0, t^m]}(t_m) \boldsymbol{\alpha}^{m, (k)} = \chi_{[t^0, t^m]}(t_0) \boldsymbol{\alpha}^0 - \sum_{r=0}^M F(\boldsymbol{\alpha}^{r, (k-1)}) \int_{t^0}^{t^M} \chi_{[t^0, t^m]}(t) \varphi_m(t) dt.$$

If we compare this equation with the fixed-point iteration of ADER (13), we can observe what the discrete methods differ in the mass matrix. However, the difference in the test functions leads to different processes in the construction of the iterative matrices. In DeC, one can not use integration by part in time, because the test functions are discontinuous. This is not a problem, since the basis functions in time are continuous and the derivatives can be applied directly there. By changing the test function also in the DeC approach, we can use the technique described in section 2, resulting in the ADER formulation.

**Conclusion 4.2.** *ADER is equivalent to DeC and vice versa, up to few details. The major difference between the two approaches presented and used in [5] and [1] is the choice of the test functions and the resulting iteration matrix.*

### 4.3 On the Accuracy of ADER

Knowing conclusion 4.2, we can finally use the DeC framework to prove the order condition for the ADER methods. Therefore, we redefine for simplicity the  $\mathcal{L}^1$  and  $\mathcal{L}^2$  operators, resulting in

$$\begin{cases} \mathcal{L}^1(\boldsymbol{\alpha}) := \boldsymbol{\alpha} - \underline{\underline{\mathbb{M}}}^{-1} r(\boldsymbol{\alpha}(t^n)) \\ \mathcal{L}^2(\boldsymbol{\alpha}) := \boldsymbol{\alpha} - \underline{\underline{\mathbb{M}}}^{-1} r(\boldsymbol{\alpha}). \end{cases} \quad (41)$$

Following the approach from [1], we need to show that

**C.1**  $\mathcal{L}^1$  is coercive

**C.2**  $\mathcal{L}^1 - \mathcal{L}^2$  is Lipschitz continuous with constant  $\beta\Delta$

**C.3** There exists a unique solution of  $\mathcal{L}^2$ , i.e.,  $\mathcal{L}^2(\underline{\alpha}^*) = 0$

in order to apply the DeC Theorem.

The next proposition shows condition **C.1**, i.e., the coercivity of the operator  $\mathcal{L}^1$ .

**Proposition 4.3** (Coercivity of  $\mathcal{L}^1$ ). *Given any  $\underline{\alpha}, \underline{\mathbf{d}}$ , such that the explicit data coincides  $\alpha(t^n) = \mathbf{d}(t^n)$ , there exists a positive  $C_0$  such that the operator  $\mathcal{L}^1$  fulfills*

$$\|\mathcal{L}^1(\underline{\alpha}) - \mathcal{L}^1(\underline{\mathbf{d}})\| \geq C_0 \|\underline{\alpha} - \underline{\mathbf{d}}\|.$$

*Proof.* We remind that the beginning states coincide for all variables, i.e.,  $\alpha(t^n) = \mathbf{d}(t^n)$ . Consider any norm  $\|\cdot\|$ , from the definition (35) we have

$$\|\mathcal{L}^1(\underline{\alpha}) - \mathcal{L}^1(\underline{\mathbf{d}})\| = \|\underline{\alpha} - \underline{\mathbf{d}}\|.$$

Therefore, we prove the statement with  $C_0 = 1$ . □

With the following proposition, we prove condition **C.2**, the Lipschitz continuity of the difference of operators.

**Proposition 4.4** (Lipschitz continuity of the  $\mathcal{L}^1 - \mathcal{L}^2$  operator). *Let  $\underline{\alpha}, \underline{\mathbf{d}}$  be in  $\mathbb{R}^{M \times I}$ . Then, the operator  $\mathcal{L}^1 - \mathcal{L}^2$  is Lipschitz continuous with constant  $C_A := \Delta t \beta$ , i.e.,*

$$\|(\mathcal{L}^1(\underline{\alpha}) - \mathcal{L}^2(\underline{\alpha})) - (\mathcal{L}^1(\underline{\mathbf{d}}) - \mathcal{L}^2(\underline{\mathbf{d}}))\| \leq C_A \|\underline{\alpha} - \underline{\mathbf{d}}\| \quad (42)$$

where  $\beta$  is independent of  $\Delta t$ .

*Proof.* First, we note that the first stages coincide for  $\underline{\alpha}$  and  $\underline{\mathbf{d}}$ , i.e.,  $\alpha(t^n) = \mathbf{d}(t^n)$ . Then, we get

$$\begin{aligned} & \|(\mathcal{L}^1(\underline{\alpha}) - \mathcal{L}^2(\underline{\alpha})) - (\mathcal{L}^1(\underline{\mathbf{d}}) - \mathcal{L}^2(\underline{\mathbf{d}}))\| \\ &= \|\underline{\alpha} - \underline{\mathbf{M}}^{-1}r(\alpha(t^n)) - \underline{\alpha} + \underline{\mathbf{M}}^{-1}r(\alpha) - \underline{\mathbf{d}} + \underline{\mathbf{M}}^{-1}r(\mathbf{d}(t^n)) + \underline{\mathbf{d}} - \underline{\mathbf{M}}^{-1}r(\underline{\mathbf{d}})\| \\ &= \|\underline{\mathbf{M}}^{-1}(r(\alpha) - r(\underline{\mathbf{d}}))\| \\ &\leq \|\underline{\mathbf{M}}^{-1}\| \|r(\alpha) - r(\underline{\mathbf{d}})\|, \end{aligned}$$

where we have just used the definition of the operators and basic linear algebra properties. Now, we have to exploit the structure of the mass matrix (10) and of the right-hand side (11). Recalling again that  $\alpha(t^n) = \mathbf{d}(t^n)$ , the difference of the two right-hand sides can be written, for every  $m = 1, \dots, M$ , as

$$\begin{aligned} & \underline{\mathbf{r}}(\underline{\alpha})_m - \underline{\mathbf{r}}(\underline{\mathbf{d}})_m \\ &= \phi_m(t^n)\alpha(t^n) - \Delta t \sum_{z=0}^Z w_z \phi_m(t_z^q) F(\underline{\phi}(t_z^q)^T \underline{\alpha}) - \phi_m(t^n)\mathbf{d}(t^n) + \Delta t \sum_{z=0}^Z w_z \phi_m(t_z^q) F(\underline{\phi}(t_z^q)^T \underline{\mathbf{d}}) \\ &= \Delta t \sum_{z=0}^Z w_z \phi_m(t_z^q) (F(\underline{\phi}(t_z^q)^T \underline{\mathbf{d}}) - F(\underline{\phi}(t_z^q)^T \underline{\alpha})), \end{aligned}$$

and using the boundedness of the basis functions  $\phi_m$  and of the weights  $w_z$  and the Lipschitz continuity of the function  $F$ , we obtain that

$$\|\underline{\mathbf{r}}(\underline{\alpha}) - \underline{\mathbf{r}}(\underline{\mathbf{d}})\| \leq \Delta t C_r \|\underline{\alpha} - \underline{\mathbf{d}}\|. \quad (43)$$

Then, the mass matrix is constant and invertible for the common points distributions, hence, the norm of its inverse does not depend on  $\Delta t$  and can be bounded by a coefficient  $C_M \in \mathbb{R}^+$ . Overall, we can write that

$$\|(\mathcal{L}^1(\underline{\alpha}) - \mathcal{L}^2(\underline{\alpha})) - (\mathcal{L}^1(\underline{\mathbf{d}}) - \mathcal{L}^2(\underline{\mathbf{d}}))\| \leq \Delta t C_M C_r \|\underline{\alpha} - \underline{\mathbf{d}}\|, \quad (44)$$

proving the statement. □

**Theorem 4.5** (Convergence of ADER - DeC). *The two operators as defined in (41) and used in the DeC algorithm (34) gives an approximate solution with order of accuracy equal to  $\min(M + 1, K)$ .*

*Proof.* Let us denote by  $\underline{\alpha}^*$  the solution of  $\mathcal{L}^2(\underline{\alpha}^*) = 0$ . We obviously have

$$\mathcal{L}^1(\underline{\alpha}^*) = \mathcal{L}^1(\underline{\alpha}^*) - \mathcal{L}^2(\underline{\alpha}^*),$$

so that with the coercivity of the  $\mathcal{L}^1$  operator

$$\left\| \underline{\alpha}^{(k)} - \underline{\alpha}^* \right\| \leq C_0 \left\| \mathcal{L}^1(\underline{\alpha}^{(k)}) - \mathcal{L}^1(\underline{\alpha}^*) \right\| \quad (45)$$

$$= \left\| \mathcal{L}^1(\underline{\alpha}^{(k-1)}) - \mathcal{L}^2(\underline{\alpha}^{(k-1)}) - \mathcal{L}^1(\underline{\alpha}^*) + \mathcal{L}^2(\underline{\alpha}^*) \right\| \quad (46)$$

$$\leq \beta \Delta t \left\| \underline{\alpha}^{(k-1)} - \underline{\alpha}^* \right\|, \quad (47)$$

where, in (45) we have used the condition **C.1** on the coercivity of  $\mathcal{L}^1$  and in (47) we have applied condition **C.2** on the Lipschitz continuity of the operator  $\mathcal{L}^1 - \mathcal{L}^2$ . This implies that after each iteration step we obtain one order of accuracy more than in the previous iteration. After  $K$  iterations, we finally get

$$\left\| \underline{\alpha}^{(K)} - \underline{\alpha}^* \right\| \leq \beta^K \Delta t^K \left\| \underline{\alpha}^{(0)} - \underline{\alpha}^* \right\|.$$

Moreover, we know that  $\underline{\alpha}^*$  is an approximation of order  $M + 1$  of the exact solution  $\underline{\alpha}^{ex}$ . So, overall we get

$$\left\| \underline{\alpha}^{(K)} - \underline{\alpha}^{ex} \right\| \leq \left\| \underline{\alpha}^* - \underline{\alpha}^{ex} \right\| + (\beta \Delta t)^K \left\| \underline{\alpha}^* - \underline{\alpha}^{(0)} \right\| \leq C^* (\Delta t^{M+1} + (\beta \Delta t)^K)$$

which proves the statement of the theorem.  $\square$

**Remark 4.6.** *In our study, we considered equidistant, Gauss–Lobatto and Gauss–Legendre nodes. For these types of nodes, we can guarantee that the mass matrix  $\underline{M}$  has full rank and, hence, it is invertible. Questions concerning the condition numbers of these matrices and related topics will be part of future research.*

## 5 Numerics

In this section, we verify our analysis by numerical simulations and also consider the stability for ADER in this context. This is up to our knowledge the first time that the stability conditions of ADER are investigated and we begin with this. Next, we compare the performance of DeC and ADER in the ODE case for linear and nonlinear scalar equations as well as ODE systems. To finish this section, we apply both approaches in a simple PDE case where the space discretization is done via a Discontinuous Galerkin method.

### 5.1 Stability Conditions

We study and compare the A-stability property of ADER and DeC. We have to mention that stability for different kind of DeC methods are already studied in the first work by Dutt et al. [6] but, here, we investigate for the first time the simplified version introduced by Abgrall [1]. Even if the differences are small, we present the results for the sake of completeness.

Consider the test problem

$$y'(t) = \lambda y(t) \quad (48)$$

$$y(0) = 1 \quad (49)$$

where  $\lambda$  is complex. In figure 2, the left picture shows the stability regions for ADER and DeC methods using Gauss–Lobatto nodes and different orders. The stability regions mapped each other and no differences can be seen. In the right picture of figure 2, we show the stability regions for both ADER and DeC methods,

using different collocation points for the subtime steps, namely, equispaced, Gauss–Legendre and Gauss–Lobatto nodes. We verify that the choice of the collocation points for the substeps does not interfere with the stability region. Furthermore, both methods seem identical for different orders (2 to 5). Further studies revealed that the different subtime step locations (Gauss–Legendre, Gauss–Lobatto and equispaced points) yielded no difference in the stability region for DeC and ADER.

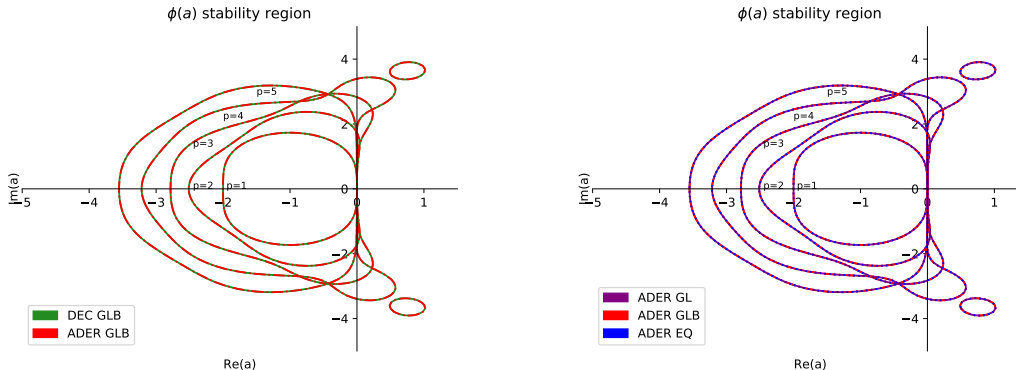


Figure 2: Stability region

## 5.2 Convergence error

In this section we report on the convergence rates of DeC and ADER, for different nodal placement of the subtime steps and for different problems.

We compute the absolute discrete  $L^2$  error taken over all the constituents (e.g. if considering systems of ODEs) and all the timesteps  $\{t^n\}_{n=0}^N$ .

$$E = \left( \frac{1}{N} \sum_{n=1}^N \frac{1}{I} \sum_{i=1}^I (y_i(t^n) - y_i^n)^2 \right)^{\frac{1}{2}}.$$

Whenever there is no analytical solution readily available, we use ODE integrators written in Julia [20] to compute a high accuracy numerical solution. These integrators use a couple of routines to select a proper numerical method for the specific type of problem. The error tolerance is set to  $10^{-16}$ .

### 5.2.1 Scalar case

We start by considering the same simple linear, scalar test case as in (48), with the initial condition, for  $t \in [0, 0.1]$ .

$$y(0) = 1.$$

Figure 3 shows the error convergence for the DeC and ADER methods, using Gauss–Lobatto nodal placement and equidistant and Gauss–Legendre nodal placements, respectively. We note that at lower orders and when the error is far enough from machine precision, all methods seem to behave the same. However, at the highest reported orders, we note that ADER EQ (denoting the equispaced nodes) does not converge with the right order. We suspected that the cause of this is the higher condition number of the mass matrix produced with equispaced nodes. It is well known that Gauss–Legendre and Gauss–Lobatto nodes have better stability properties. DeC is not affected by this particular problem because it does not require a mass matrix. Another problem that may arise are the negative weights related to the equispaced nodes. They are

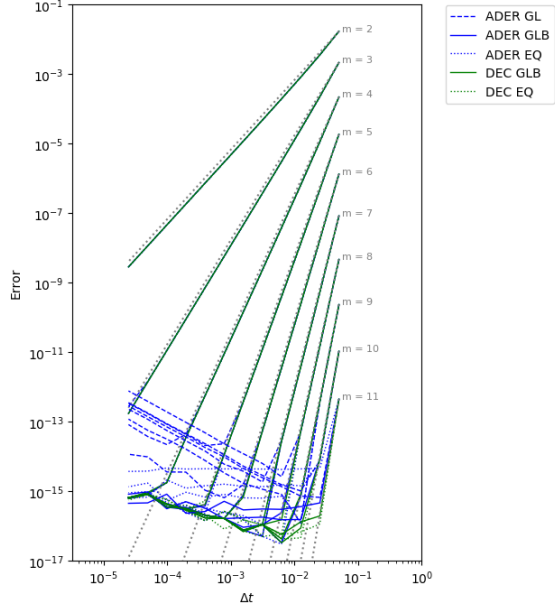


Figure 3: Convergence curves for ADER and DeC, varying the approximation order and collocation of nodes for the subimesteps for a scalar linear ODE (48).

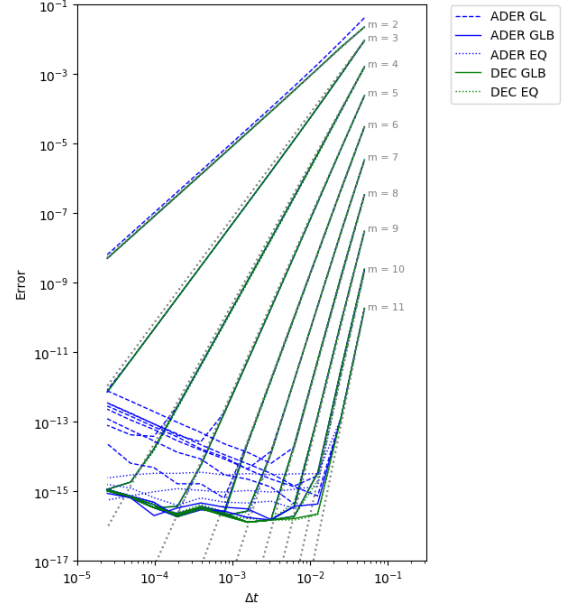


Figure 4: Convergence curves for ADER and DeC, varying the approximation order and collocation of nodes for the subimesteps for a scalar nonlinear ODE (50).

present from ninth order on and also the classical Runge phenomena can appear. This is also true, of course, for ADER EQ. Furthermore, ADER GL (denoting Gauss–Legendre nodes) also shows a strange behavior at high orders and high resolutions. We believe this is because of the required extrapolatory step to compute the solution at  $t^{n+1}$ , only necessary when using nodes that do not include the boundaries of the interval. The difference between ADER GLB and DeC GLB seem to be negligible. Next, we consider the nonlinear scalar problem

$$\begin{aligned} y'(t) &= -k|y(t)|y(t) \\ y(0) &= 1, \end{aligned} \tag{50}$$

with  $k = 1$  and  $t \in [0, 0.1]$ .

Figure 4 shows the error convergence for the DeC and ADER methods, using Gauss–Lobatto nodal placement, equidistant and Gauss–Legendre nodal placements, respectively. The behaviour of the different schemes is similar to the one reported in the scalar linear case.

### 5.2.2 Systems

We consider a simple biological model that models the transfer of biomass, given by a set of linear ODEs

$$\begin{aligned} y_1'(t) &= -y_1(t) + 3y_2(t) \\ y_2'(t) &= -3y_2(t) + 5y_3(t) \\ y_3'(t) &= -5y_3(t), \end{aligned} \tag{51}$$

with the initial conditions

$$(y_1(0), y_2(0), y_3(0)) = (0, 0, 10),$$

and we let  $t \in [0, 1]$ .

The analytical solution is given as

$$\begin{aligned} y_1(t) &= \frac{15}{8} y_3(0) (e^{-5t} - 2e^{-3t} + e^{-t}) \\ y_2(t) &= \frac{5}{2} y_3(0) (e^{-5t} + e^{-3t}) \\ y_3(t) &= y_3(0) e^{-5t}. \end{aligned}$$

In figure 5, we show the error convergence for the DeC and ADER methods using different nodal placements. Again, everything is as expected and we obtain the desired convergence rates.

### Lotka–Volterra equations

In the last test for ODEs, we consider the Lotka–Volterra equations [3] that describe the dynamics of a two–species system in which one is a predator and the other its prey. The following nonlinear equations describe the dynamics of the prey ( $y_1$ ) and the predator ( $y_2$ ):

$$\begin{aligned} y_1'(t) &= \alpha y_1(t) - \beta y_1(t) y_2(t) \\ y_2'(t) &= -\gamma y_2(t) + \delta y_1(t) y_2(t) \end{aligned} \tag{52}$$

where  $\alpha$  is the growth rate of the prey,  $\beta$  the predation rate,  $\delta$  the predator food conversion efficiency and  $\gamma$  the predator mortality.

We use the following initial conditions and parameters

$$\begin{aligned} (y_1(0), y_2(0)) &= (1, 2) \\ (\alpha, \beta, \delta, \gamma) &= (1, 0.2, 0.5, 0.2), \end{aligned} \tag{53}$$

and we let  $t \in [0, 5]$ .

Again, figure 6 shows the error convergence for the DeC and ADER methods, using different nodal placements. In figures 7 and 8, we show the solution to the initial conditions (53) and for  $t \in [0, 100]$ , comparing the performance of ADER and DEC (with Gauss–Lobatto nodes) at different orders and resolutions.

### 5.2.3 PDE case

We consider the advection equation, a 1-dimensional scalar, linear partial differential equation, given by the initial value problem

$$\begin{aligned} \partial_t u + a \partial_x u &= 0, \quad x \in \mathbb{R}, \quad t > 0 \\ a &\in \mathbb{R} \\ u(x, 0) &= u_0(x), \quad x \in \mathbb{R}. \end{aligned} \tag{54}$$

We consider the initial conditions

$$u_0(x) = \sin(2\pi x) \quad x \in [0, 1].$$

We discretize the equation with the method of lines. The space operator is discretized with a Flux Reconstruction (FR) method, whereas the time integration is performed with ADER or DEC (using the different collocation points for the subtime steps). From figure 9, we observe the appropriate convergence rates at  $T = 1$ .



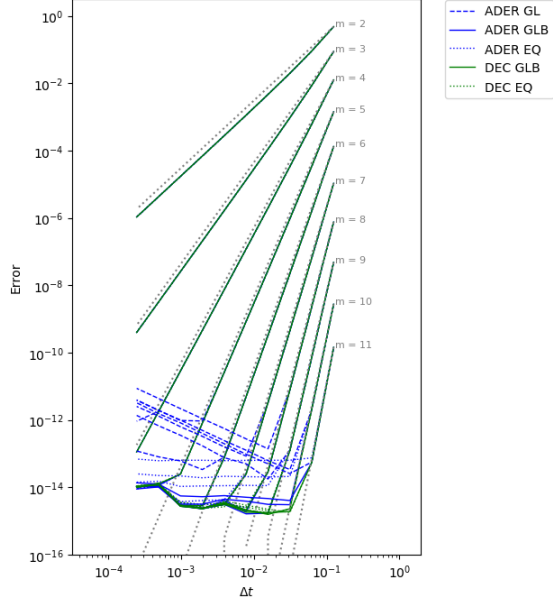


Figure 5: Convergence curves for ADER and DeC, varying the approximation order and collocation of nodes for the subtimesteps for the system of linear ODEs (51).

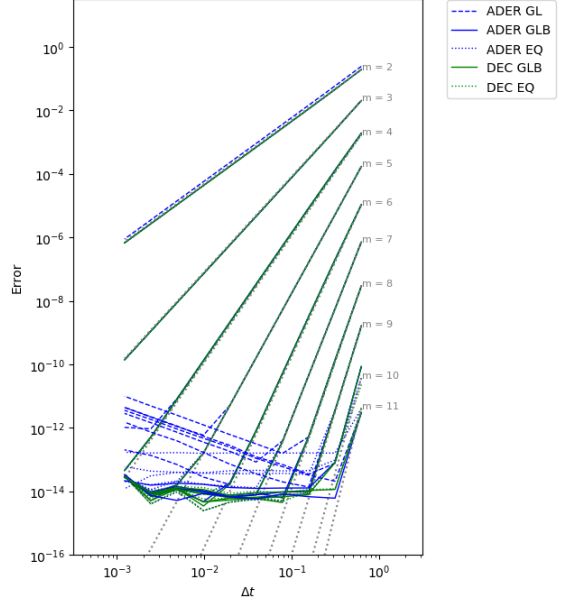


Figure 6: Convergence curves for ADER and DeC, varying the approximation order and collocation of nodes for the subtimesteps for the system of nonlinear ODEs (52).

Finally, we consider the Burgers' equation, a 1-dimensional scalar, nonlinear partial differential equation, given by the initial value problem

$$\begin{aligned} \partial_t u + u \partial_x u &= 0, & x \in \mathbb{R}, & t > 0 \\ u(x, 0) &= u_0(x), & x \in \mathbb{R}. \end{aligned} \quad (55)$$

We consider the initial conditions

$$u_0(x) = \tanh(10x - 5) \quad x \in [0, 1],$$

with  $t \in [0, 0.05]$ .

Again, the space operator is discretized with a FR method, whereas the time integration is performed with ADER or DEC (using the different collocation points for the subtimesteps). From figures 11 and 12, we observe the appropriate convergence rates, with no noticeable differences between the different collocation points. The reference solution is a high resolution numerical solution, interpolated at the necessary spatial points to compute the error. It is to note that the solution in the ADER case was more stable when the update was performed in the following way:

$$u(t^{n+1}) = u(t^n) - \Delta t \partial_x \int_{T^n} f(\underline{\phi}(t)^T \underline{\alpha}^{(k+1)}),$$

rather than

$$u(t^{n+1}) = \underline{\phi}(1)^T \underline{\alpha}^{(k+1)}.$$

This made no significant difference for the linear advection case.

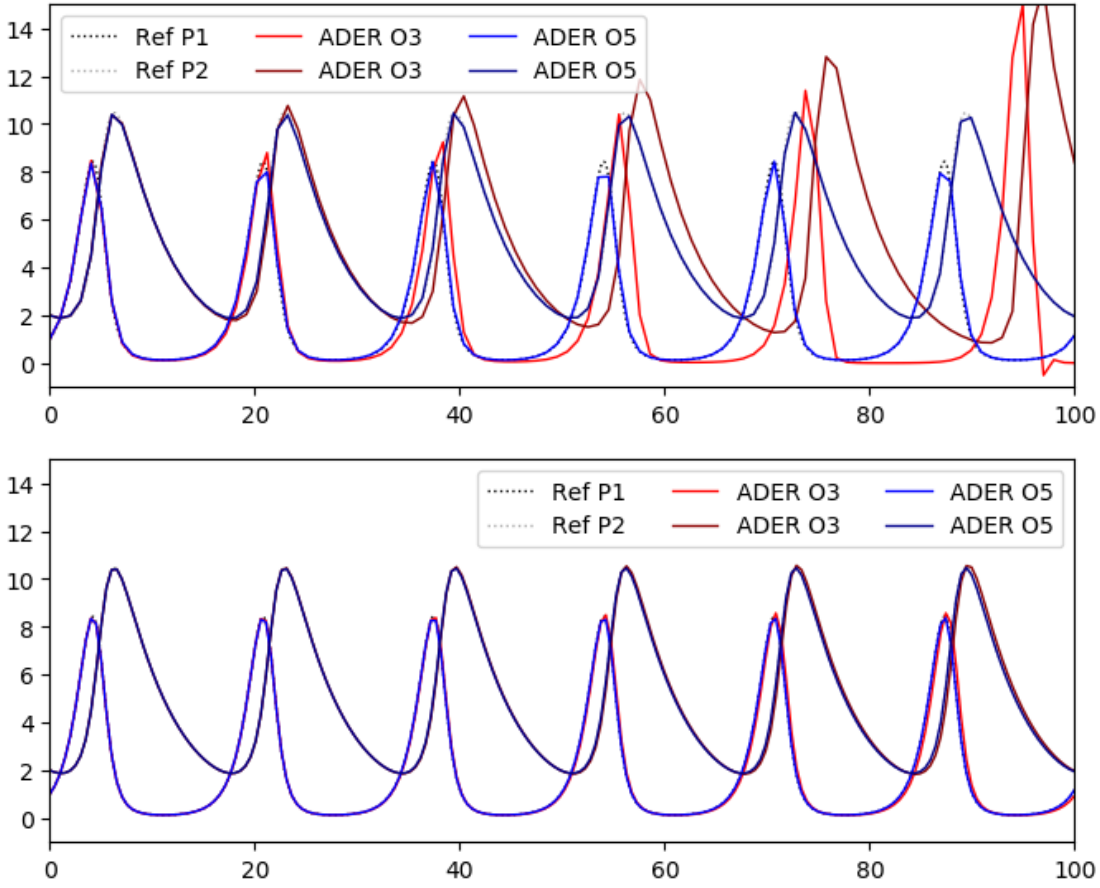


Figure 7: Numerical solution of the Lotka-Volterra system (52), using initial conditions (53) using ADER with Gauss-Lobatto nodes at different orders. The top figure uses a timestep  $\Delta T = 1$ , the bottom figure  $\Delta T = 0.5$ .

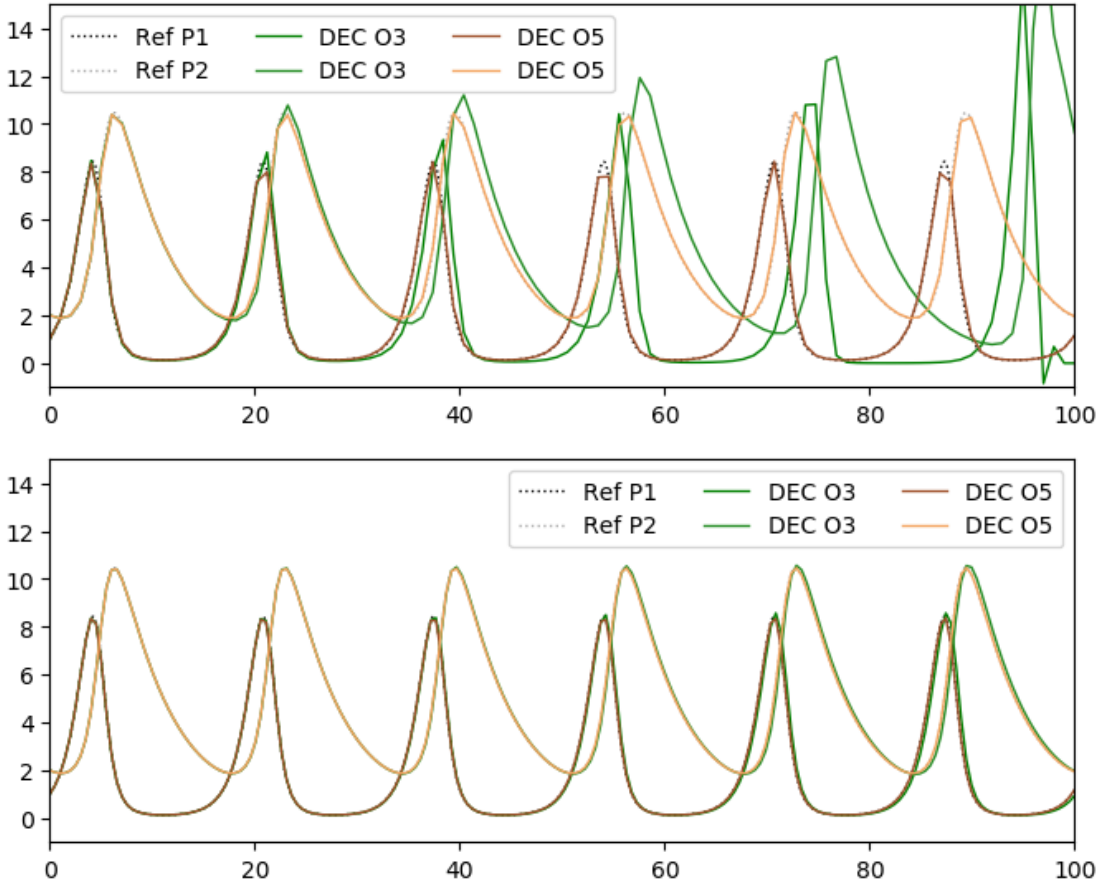


Figure 8: Numerical solution of the Lotka-Volterra system (52), using initial conditions (53) using DEC with Gauss-Lobatto nodes at different orders. The top figure uses a timestep  $\Delta T = 1$ , the bottom figure  $\Delta T = 0.5$ .

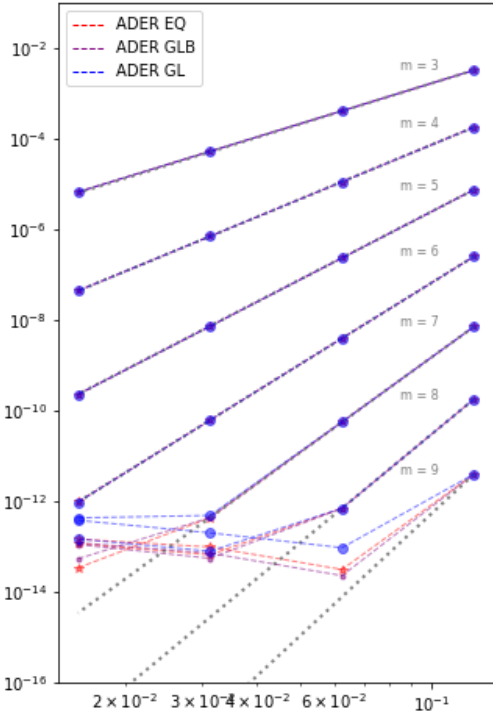


Figure 9: Convergence curves for ADER, varying the approximation order and collocation of nodes for the subtime steps for the linear advection equation (54).

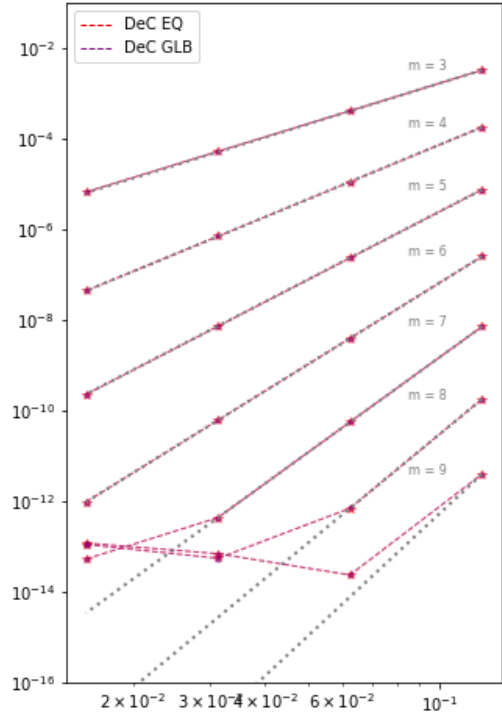


Figure 10: Convergence curves for DeC, varying the approximation order and collocation of nodes for the subtime steps for the linear advection equation (54).

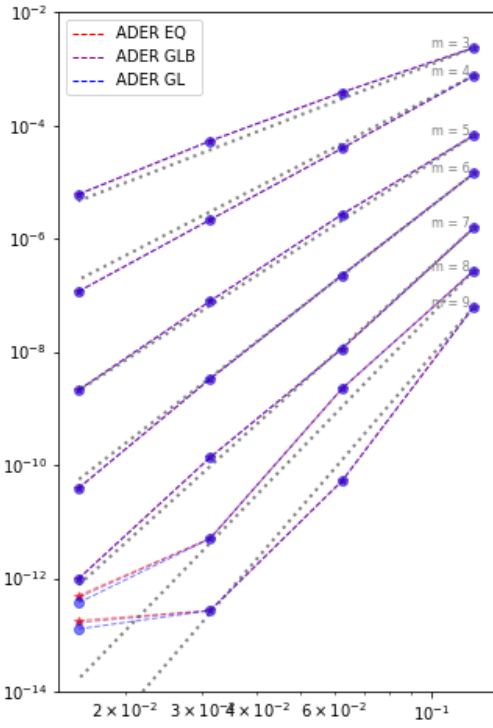


Figure 11: Convergence curves for ADER using SD for the space discretization for the Burgers' Equation (55).

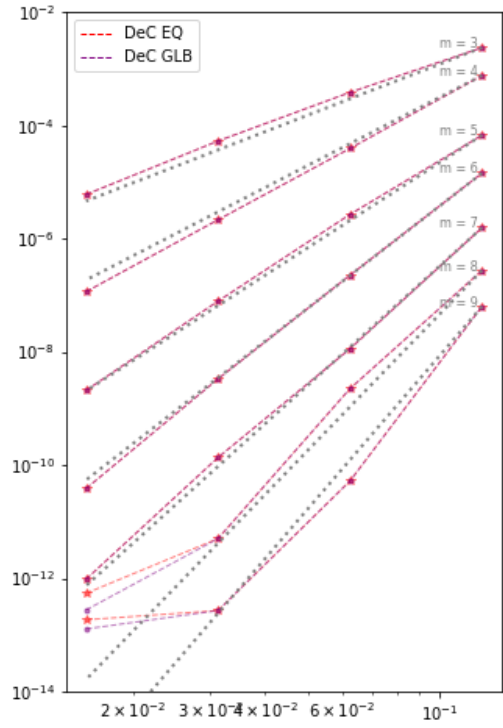


Figure 12: Convergence curves for DeC using SD for the space discretization for the Burgers' Equation (55).

## 6 Summary and Outlook

In this paper, we have demonstrated the connection between the DeC framework and the ADER approach. In particular, we showed that ADER can be interpreted as DeC, as well as DeC is equivalent to ADER up to a choice of test functions.

Since we embed ADER in the theoretical DeC framework, we were able to demonstrate theoretical results for ADER, e.g. how many iterations are needed to obtain the desired order, extending the results of [11]. Further, we investigate the stability regions for both approaches which supports and verifies our theoretical consideration.

This connection was explored numerically on a variety of tests, with ODEs and PDEs. At the same time, we also studied the influence of the choice of collocation points in time and verified that there was not much of a difference, except that for very high orders, equidistant nodes seem to lose the convergence order and we attribute this to the fact that the condition number of the mass matrix degrades as the order is increased. This fact affects ADER but not DeC, as the latter bypasses the mass matrix by construction. Furthermore, at high orders, we also observed that the use of Gauss–Legendre collocation points, which requires a step of extrapolation in the ODE case, seemed to have a worse performance than when using Gauss–Lobatto nodes. We hope that, with this paper, the modern ADER approach and DeC become clearer to the community and that it becomes clear that these methods are very similar. Furthermore, since we have provided some theoretical background for ADER as a time–integration scheme, many further extensions are possible and new questions can be asked: for example, what is the relation between ADER and RK methods, as it was already done for DeC in [4]. Another possibility is to rewrite ADER in SSP formulation, in the spirit of [14], or to build ADER schemes which are positivity preserving and conservative by using a Patankar trick [10, 19]. Finally, extensions to relaxation approaches introduced by Ketcheson et al. [12, 21] are also possible to construct entropy conservative ADER schemes, where this is already work in progress for the DeC approach.

Finally, in spirit of open science, all codes used to produce this paper are available in [9].

## Acknowledgements

P. Öffner has been funded by the UZH Postdoc Grant. Davide Torlo is supported by ITN ModCompShock project funded by the European Unions Horizon 2020 research and innovation program under the Marie Skłodowska-Curie grant agreement No 642768. M. Han Veiga acknowledges financial support from MIDAS.

## References

- [1] R. Abgrall. High order schemes for hyperbolic problems using globally continuous approximation and avoiding mass matrices. *Journal of Scientific Computing*, 73(2):461–494, Dec 2017.
- [2] R. Abgrall and D. Torlo. Asymptotic preserving deferred correction residual distribution schemes. *arXiv preprint arXiv:1811.09284*, 2018.
- [3] N. Bacaer. *A Short History of Mathematical Population Dynamics*. 01 2011.
- [4] A. Christlieb, B. Ong, and J.-M. Qiu. Integral deferred correction methods constructed with high order runge-kutta integrators. *Mathematics of Computation*, 79(270):761–783, 2010.
- [5] M. Dumbser, D. S. Balsara, E. F. Toro, and C.-D. Munz. A unified framework for the construction of one-step finite volume and discontinuous galerkin schemes on unstructured meshes. *Journal of Computational Physics*, 227(18):8209–8253, 2008.
- [6] A. Dutt, L. Greengard, and V. Rokhlin. Spectral Deferred Correction Methods for Ordinary Differential Equations. *BIT Numerical Mathematics*, 40(2):241–266, 2000.

- [7] J. Glaubitz and P. Öffner. Stable discretisations of high-order discontinuous galerkin methods on equidistant and scattered points. *Applied Numerical Mathematics*, 2020.
- [8] J. Glaubitz, P. Öffner, and T. Sonar. Application of modal filtering to a spectral difference method. *Mathematics of Computation*, 87(309):175–207, 2018.
- [9] M. Han Veiga, P. Öffner, and D. Torlo. ADER and DeC implementations. [https://git.math.uzh.ch/abgrall\\_group/dec-is-ader](https://git.math.uzh.ch/abgrall_group/dec-is-ader), 02 2020.
- [10] J. Huang and C.-W. Shu. Positivity-preserving time discretizations for production–destruction equations with applications to non-equilibrium flows. *Journal of Scientific Computing*, 78(3):1811–1839, 2019.
- [11] H. Jackson. On the eigenvalues of the ader-weno galerkin predictor. *Journal of Computational Physics*, 333:409 – 413, 2017.
- [12] D. I. Ketcheson. Relaxation runge-kutta methods: Conservation and stability for inner-product norms. *SIAM J. Numerical Analysis*, 57:2850–2870, 2019.
- [13] P. Lax and B. Wendroff. Systems of conservation laws. *Communications on Pure and Applied Mathematics*, 13(2):217–237, 1960.
- [14] Y. Liu, C.-W. Shu, and M. Zhang. Strong stability preserving property of the deferred correction time discretization. *Journal of Computational Mathematics*, pages 633–656, 2008.
- [15] Y. Liu, M. Vinokur, and Z. Wang. Discontinuous spectral difference method for conservation laws on unstructured grids. In *Computational fluid dynamics 2004*, pages 449–454. Springer, 2006.
- [16] M. L. Minion. Semi-implicit spectral deferred correction methods for ordinary differential equations. *Commun. Math. Sci.*, 1(3):471–500, 09 2003.
- [17] J. Nordström and T. Lundquist. Summation-by-parts in time. *Journal of Computational Physics*, 251:487–499, 2013.
- [18] P. Öffner and H. Ranocha. Error boundedness of discontinuous galerkin methods with variable coefficients. *Journal of Scientific Computing*, 79(3):1572–1607, 2019.
- [19] P. Öffner and D. Torlo. Arbitrary high-order, conservative and positive preserving patankar-type deferred correction schemes. *Applied Numerical Mathematics*, 153:15–34, 2020.
- [20] C. Rackauckas and Q. Nie. Differentialequations. jl—a performant and feature-rich ecosystem for solving differential equations in julia. *Journal of Open Research Software*, 5(1), 2017.
- [21] H. Ranocha, M. Sayyari, L. Dalcin, M. Parsani, and D. I. Ketcheson. Relaxation runge-kutta methods: Fully-discrete explicit entropy-stable schemes for the euler and navier-stokes equations. *arXiv preprint arXiv:1905.09129*, 2019.
- [22] S. J. Ruuth and R. J. Spiteri. Two barriers on strong-stability-preserving time discretization methods. *J. Sci. Comput.*, 17(14):211220, Dec. 2002.
- [23] S. T., M. C. D., and T. E. F. ADER: A High-Order Approach for Linear Hyperbolic Systems in 2D. *Journal of Scientific Computing*, 17(1):231240, 2002.
- [24] V. A. Titarev and E. F. Toro. Ader: Arbitrary high order godunov approach. *Journal of Scientific Computing*, 17(1-4):609–618, 2002.
- [25] E. Toro. *Riemann Solvers and Numerical Methods for Fluid Dynamics: A Practical Introduction*. Springer Berlin Heidelberg, 2009.

- [26] E. Toro, R. Millington, and L. Nejad. Towards very high order godunov schemes. In *Godunov methods*, pages 907–940. Springer, 2001.
- [27] E. F. Toro and V. A. Titarev. Solution of the generalized riemann problem for advection&#x2013;reaction equations. *Proceedings of the Royal Society of London. Series A: Mathematical, Physical and Engineering Sciences*, 458(2018):271–281, 2002.
- [28] G. Wanner and E. Hairer. *Solving ordinary differential equations II*. Springer Berlin Heidelberg, 1996.
- [29] O. Zanotti, F. Fambri, M. Dumbser, and A. Hidalgo. Space–time adaptive ader discontinuous galerkin finite element schemes with a posteriori sub-cell finite volume limiting. *Computers & Fluids*, 118:204–224, 2015.